Electronic and atomic structures of quasi-one-dimensional $K_{0.3}MoO_3$

C. H. Huang, J. C. Jan, J. W. Chiou, H. M. Tsai, C. W. Pao, C. H. Du, and W. F. Pong[a)]
Department of Physics, Tamkang University, Tamsui 251, Taiwan

M.-H. Tsai
Department of Physics, National Sun Yat-Sen University, Kaohsiung 804, Taiwan

M. T. Tang, J. J. Lee, and J. F. Lee
National Synchrotron Radiation Research Center, Hsinchu 300, Taiwan

(Received 2 December 2004; accepted 15 February 2005; published online 30 March 2005)

The electronic and atomic structures of quasi-one-dimensional blue bronze $K_{0.3}MoO_3$ were investigated by polarization-dependent O *K*-edge x-ray absorption near-edge structure (XANES) and Mo *K*-edge extended x-ray absorption fine structure (EXAFS) measurements at various temperature and applied voltages. The O *K*-edge XANES spectra suggest that the number of unoccupied O $2p-$Mo $4d$ hybridized states increases and decreases with temperature, respectively, below and above a critical temperature of 180 K. The along *b*-axis electric current measurements show a threshold applied voltage, beyond which the current increases rapidly. The Mo *K*-edge EXAFS measurements show that the Mo–O bond lengths are insensitive to the temperature even beyond 180 K. © *2005 American Institute of Physics*. [DOI: 10.1063/1.1897437]

Blue bronze $K_{0.3}MoO_3$ exhibits quasi-one-dimensional (1D) electron transport property and a metal–semiconductor transition to a charge-density-wave (CDW) phase at 180 K[1,2] and has been investigated extensively.[1–13] Of particular interests are the occurrence of the CDW and the corresponding dynamical properties, which depend strongly on the temperature and the driving force.[3,4] The overall dynamical CDW characteristics were specified in the order of increasing driving force as (i) deformed solid at rest, (ii) plastic flow or creep, and (iii) sliding.[3,4] Thorne[5] and Scheidl and Vinokur[6] reported dynamic phase diagrams with respect to temperatures and external fields. The anisotropic electrical resistivity of $K_{0.3}MoO_3$ has been found to be an order of magnitude larger in the plane of the layers than in the *b* direction,[7] and to depend strongly on temperature.[8] In this work, a systematic study of local electronic and atomic structures at various temperatures and driving forces has been performed to elucidate the dynamic property of 1D $K_{0.3}MoO_3$.

The polarization-dependent O *K*-edge x-ray absorption near-edge structure (XANES) and Mo *K*-edge extended x-ray absorption fine structure (EXAFS) spectra at various temperatures and dc electrical voltages were obtained using a high-energy spherical grating monochromator beamline at the National Synchrotron Radiation Research Center, Hsinchu, Taiwan, and a BL12B2 beamline at Spring-8, Japan, using the fluorescence mode, respectively. The $K_{0.3}MoO_3$ single crystal was grown using a temperature gradient flux technique. The orientation was characterized by x-ray diffraction.[9] A rectangular piece of the crystal with an area of $\sim 2\times 3$ mm^2 was prepared. The sample was mounted in a continuous-flow-type helium cryostat for temperature-dependent measurements. The longer side of the rectangle was aligned with the *b* axis of the crystal. Two platinum wire electrodes were attached to the surface of the sample in the contact regions using silver pastes. A Keithely 2400 source meter was applied to generate the driving dc electrical voltage and the current–voltage curve was measured in a two-probe setup.

Figure 1 displays the normalized O *K*-edge XANES spectra of $K_{0.3}MoO_3$ obtained at temperatures from 100 to 300 K. The upper part of the inset in Fig. 1 shows the experimental geometry, where $\boldsymbol{E}$ is the polarization of the incoming photons and θ is the incidence angle. The inset of Fig. 1 presents magnified near-edge features at temperatures of 100, 180, and 300 K at $\theta=0°$. The dotted line in Fig. 1 is a best-fitted Gaussian curve representing the background intensity. The O *K*-edge XANES spectra reflect transitions from the O $1s$ core state to the unoccupied O $2p$-derived states and states of neighboring atoms, which have

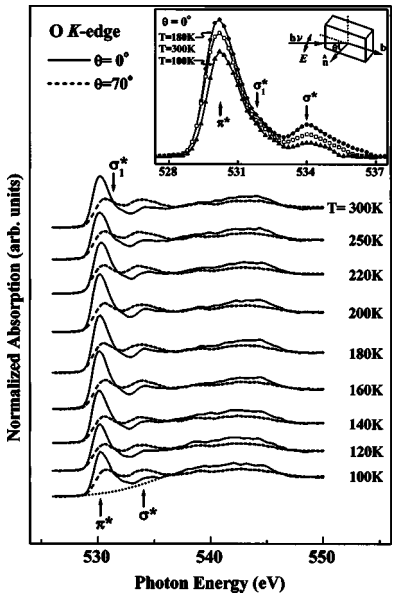

FIG. 1. This figure displays polarization-dependent O *K*-edge XANES spectra of $K_{0.3}MoO_3$ between 100 and 300 K. The dotted line represents a best-fitted Gaussian shape background. The upper part of the inset presents the XANES experimental geometry. The inset shows magnified π^* and σ^* features at $T=100$, 180, and 300 K after background subtraction.

[a)]Author to whom correspondence should be addressed; electronic mail: wfpong@mail.tku.edu.tw

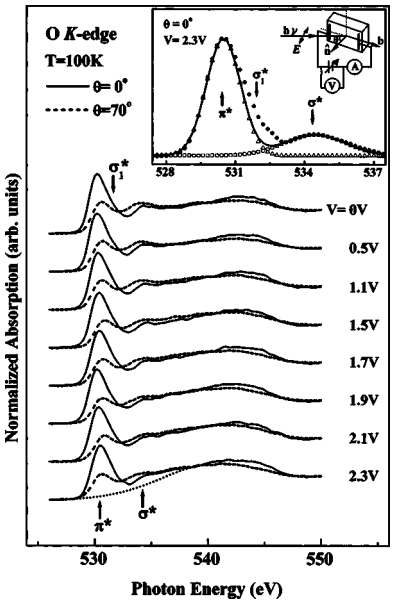

FIG. 2. This figure displays *V*-dependent O *K*-edge XANES spectra of $K_{0.3}MoO_3$ at 100 K. The upper part of the inset shows XANES experimental geometry and the electrical circuit. The inset shows magnified π^* and σ^* features at 100 K ($\theta=0°$ and $V=2.3$ V) after background subtraction. Solid lines are fitted with two Gaussian peaks indicated by open rectangles and triangles. Filled circles represent experimental data.

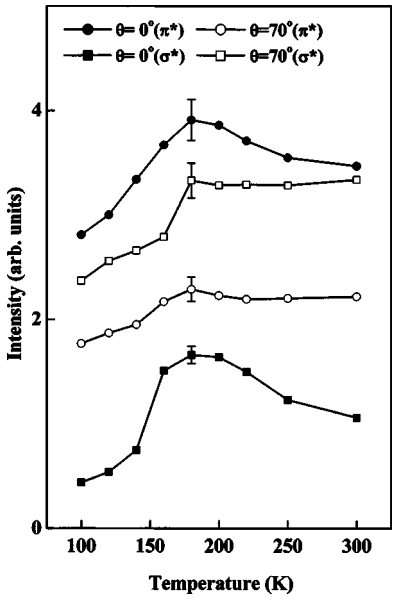

FIG. 3. This figure plots the integrated intensities of π^* and σ^* features in O *K*-edge XANES spectra as functions of *T*.

p-symmetry components projected on the O sites. The two prominent features near 530.2 and 534.1 eV are known to be associated with unoccupied π^* and σ^* bands formed by hybridization between O $2p_\pi$ and Mo $4dt_{2g}$ states and between O $2p_\sigma$ and Mo $4de_g$ states,[10–12] respectively. A weak feature, σ_1^*, attributable to a theoretical energy level of $K_{0.3}MoO_3$ is also found.[12] Figure 1 indicates that the intensity of the π^* (σ^*) feature at $\theta=0°$ is always larger (smaller) than that at $\theta=70°$ for the various temperatures considered. The MoO_6 octahedron chains are parallel to the monoclinic *b* axis in $K_{0.3}MoO_3$. Four Mo–O bonds lie in the central plane and two Mo–O bonds are along the *b* axis, which can be called σ bonds (or central-plane bonds) and the π bonds (or *b*-axis bonds), respectively. The π and σ bonds are preferentially probed at small and large incidence angles, respectively, because the polarization of photons is parallel to π and σ bonds at small and large incident angles, respectively. Thus, the dependence of the intensity on the incident angle is an evidence of high anisotropy in the electronic structure.

Figure 2 displays polarization-dependent O *K*-edge XANES spectra of $K_{0.3}MoO_3$ obtained at various dc electrical voltages, *V*, from 0 to 2.3 V at $T=100$ K. The upper part of the inset schematically depicts the experimental setup. The inset of Fig. 2 presents a magnified view to better resolve π^* and σ^* features at $\theta=0°$, $V=2.3$ V and $T=100$ K. Two best-fitted Gaussian functions are used to represent π^* and σ^* features in the inset of Fig. 2 using the spectrum of $V=2.3$ V and $T=100$ K as an example. Here, the σ_1^* feature is not considered. Figures 3 and 4 plot the integrated intensities of π^* and σ^* features as functions of temperature and dc electrical voltage at $T=100$ K, respectively. Figure 4 also plots the electrical current as a function of applied voltage. The integrated intensities of π^* and σ^* features increase rapidly from 100 to 180 K and then decrease slowly up to 300 K for $\theta=0°$. At $\theta=70°$ the intensities of π^* and σ^* features increase less rapidly from 100 to 180 K and then remain almost constant up to 300 K.

The rapid increase of π^*- and σ^*-feature intensities for $\theta=0°$ and for $T<180$ K indicates a rapid increase of the number of unoccupied O $2p$ states or a rapid decrease of the number of occupied O $2p$ states, which indicates an increase of hole concentration and implies that $K_{0.3}MoO_3$ is semiconducting below 180 K. Since photon polarizations are parallel with the *b* axis for $\theta=0°$, the decrease of π^*- and σ^*-feature intensities beyond 180 K shows that the number of unoccupied O $2p$ states oriented along the *b* axis decreases, which may be due to an increase of the chemical potential because these states are in the vicinity of the chemical potential/Fermi level. Another possibility is the decrease of Mo–O hybridization resulted from an increase of the Mo–O bond length. However, the Mo *K*-edge EXAFS results to be described later show that Mo–O bond lengths are insensitive to the temperature. The near constant π^*- and σ^*-feature inten-

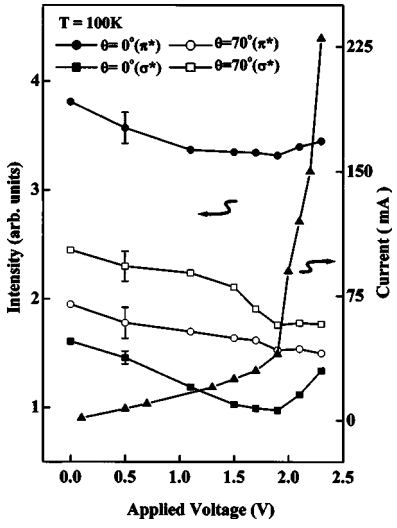

FIG. 4. This figure plots the integrated intensities of π^* and σ^* features in O *K*-edge XANES spectra as functions of *V* at $T=100$ K, $\theta=0°$ and 70°. The electrical current data are shown by filled triangles.

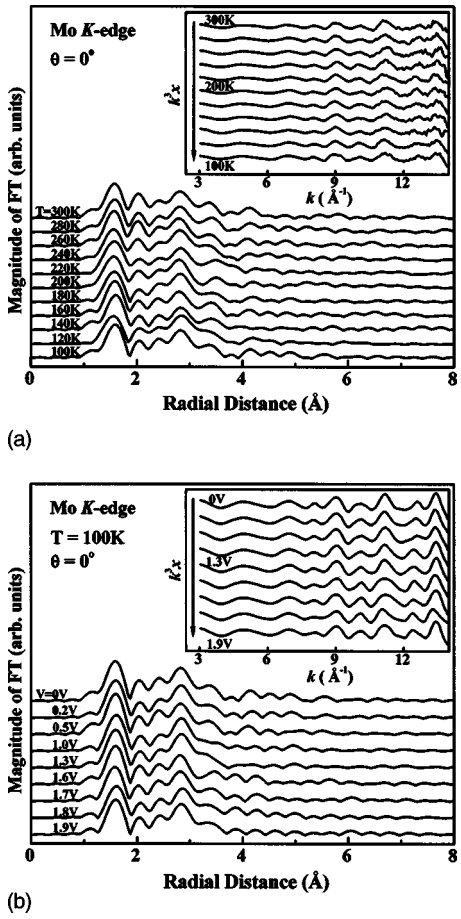

FIG. 5. (a) and 5(b) show the magnitudes of the Fourier transform of EXAFS $k^3\chi(k)$ spectra from $k=3.5$ to 12.5 $Å^{-1}$ at various temperatures and various dc voltages, respectively. The inset plots the Mo *K*-edge EXAFS oscillation $k^3\chi$ data.

sities for $\theta=70°$ above 180 K is understandable because the orientation of these O $2p$ orbitals are perpendicular to the *b* axis and these states are further away from the chemical potential/Fermi level.

Figure 4 plots the dependence of the intensities of π^* and σ^* features on V at 100 K. The intensities decrease monotonically as *V* increases from 0 to 1.9 V. The intensities increase for $\theta=0°$ and remain more or less constant for $\theta=70°$ beyond 1.9 V. The decrease of π^*- and σ^*-feature intensities with the increase of *V* is due to the increase of electron energies gained from the electric field, which reduces the number of unoccupied O $2p$ states. Above 1.9 V, the increase of π^*- and σ^*-feature intensities for $\theta=0°$ may be interpreted as the shortening of some of the Mo–O bonds driven by the field along the *b* axis, which increases Mo–O hybridization and consequently the number of unoccupied antibonding states. Figure 4 shows that the current increases approximately linear up to about 1.9 V and then increases rapidly beyond. The rapid increase above 1.9 V can be interpreted as the onset of the sliding of the CDW.[5] However, the mere existence of a small energy gap can also give rise to a rapid increase of current beyond a threshold voltage.

Figures 5(a) and 5(b) plot *T*- and *V*- (at $T=100$ K) dependent EXAFS oscillation $\chi(k)$ weighted by k^3 for the Mo *K* edge (shown in the insets) and the corresponding Fourier transform (FT) of the $k^3\chi$ data, respectively, at $\theta=0°$. The *T*-dependent measurements were intended to obtain information about electron-phonon couplings, which was proposed by previous researchers to be the cause of the CDW formation and CDW-metal phase transition. The *V*-dependent measurements were intended to understand the dynamic property of the CDW, which is supposedly associated with the change of the local atomic structure in $K_{0.3}MoO_3$. The positions of the first main peaks in the FT spectra shown in Figs. 5(a) and 5(b) correspond to a mixture of two nearest-neighbor Mo–O bond lengths (approximately 1.9–2.0 Å)[13] along the *b* axis. All the peaks in the FT spectra shown in Fig. 5(a) appear to be located approximately at the same position and their heights and full widths at half maximum are insensitive to *T* from 100 to 300 K. This finding shows that Mo–O bond lengths remain almost the same. The *V*-dependent FT spectra presented in Fig. 5(b) show that Mo–O bond lengths in $K_{0.3}MoO_3$ are insensitive to *V* up to 1.9 V. These EXAFS spectra differ noticeably only for radial distances beyond ~3.3 Å. Under an applied electric field, $K_{0.3}MoO_3$ was proposed to undergo deformation-to-creep-to-slide dynamic phase transitions.[3–5] Deformation, creeping, and sliding all involve modification of local atomic structure and Mo–O bond lengths. In the sliding process, bond length distribution was envisioned to be periodically altered (Fig. 3 of Ref. 5). Thus, the observed similarity of the EXAFS spectra for *T* up to 300 K and *V* up to 1.9 V suggest that either the periodic distortion of the MoO_6 octahedron-chain along the *b* axis be small or the distortion be mainly on the bond angles.

In summary, polarization-dependent O *K*-edge XANES measurements reveal that the electronic structure of $K_{0.3}MoO_3$ is anisotropic and that the number of O $2p-$Mo $4d$ hybridized states increases and decreases with temperature, respectively, below and above 180 K. The along *b*-axis electric current measurements show a threshold voltage, beyond which the current increases rapidly. Mo *K*-edge EXAFS measurements show that the Mo–O bond lengths are insensitive to the temperature even beyond the critical temperature of 180 K.

The author (W.F.P.) would like to thank the National Science Council of R.O.C. for financially supporting this research under Contract No. NSC 92-2112-M-032-025.

[1] *Low Dimensional Electronic Properties of Molybdenum Bronzes and Oxides*, edited by C. Schlenker (Kluwer, Dordrecht, 1989).
[2] G. Grüner, Rev. Mod. Phys. **60**, 1129 (1988); G. Grüner, *Density Waves in Solids* (Addison-Wesley, Longmans, MA, 1994).
[3] L. Balents and M. P. A. Fisher, Phys. Rev. Lett. **75**, 4270 (1995).
[4] N. Ogawa, A. Shiraga, R. Kondo, S. Kagoshima, and K. Miyano, Phys. Rev. Lett. **87**, 256401 (2001); N. Ogawa, Y. Murakami, and K. Miyano, Phys. Rev. B **65**, 155107 (2002).
[5] R. E. Thorne, Phys. Today **49**, 42 (1996).
[6] S. Scheidl and V. M. Vinokur, Phys. Rev. E **57**, 2574 (1998).
[7] R. Brusetti, B. K. Chakraverty, J. Devenyi, J. Dumas, J. Marcus, and C. Schlenker, in *Recent Development in Condensed Matter Physics*, edited by J. T. Deeveese, L. F. Lemmens, V. E. Van Doren, and J. van Royen (Plenum, New York, 1981), Vol. 2.
[8] W. Brütting, P. H. Nguyen, W. Riess, and G. Paasch, Phys. Rev. B **51**, 9533 (1995).
[9] C. H. Du, M. T. Tang, and S. L. Chang (unpublished).
[10] L. C. Duda, J. H. Guo, J. Nordgren, C. B. Stagarescu, K. E. Smith, W. McCarroll, K. Ramanujachary, and M. Greenblatt, Phys. Rev. B **56**, 1284 (1997).
[11] M. Sing, R. Neudert, H. von Lips, M. S. Golden, M. Knupfer, J. Fink, R. Claessen, J. Mücke, H. Schmitt, S. Hüfner, B. Lommel, W. Aßmus, Ch. Jung, and C. Hellwig, Phys. Rev. B **60**, 8559 (1999).
[12] G. Travaglini, P. Wachter, J. Marcus, and C. Schlenker, Solid State Commun. **37**, 599 (1981).
[13] M.-H. Whangbo and L. F. Schneemeyer, Inorg. Chem. **25**, 2424 (1986).